Electronic Supporting Information (ESI)

$KBa_3M_2F_{14}Cl$ (M = Zr, Hf): novel short-wavelength metal mixed halides with largest second-harmonic generation responses contributed by mixed functional moieties

Mei Yan,[‡a] Chun-Li Hu,[‡b] Ru-Ling Tang,[*a] Wen-Dong Yao,[a] Wenlong Liu,[a] and Sheng-Ping Guo[*a]

a School of Chemistry and Chemical Engineering, Yangzhou University, Yangzhou, Jiangsu 225002, P. R. China

b State Key Laboratory of Structural Chemistry, Fujian Institute of Research on the Structure of Matter, Chinese Academy of Sciences, Fuzhou, Fujian, 350002, China

Corresponding authors: rltang@yzu.edu.cn, spguo@yzu.edu.cn

‡ Mei Yan and Chun-Li Hu contributed equally.

CONTENTS

1. Experimental section.

Caution: Hydrofluoric acid is a highly toxic and corrosive substance. Proper protective equipment must be worn by users during the experimental process.

1.1 Reagents. KCl (AR, 99 %, Macklin), $BaCl_2 \cdot 2H_2O$ (AR, 99.99 %, Aladdin), ZrF_4 (AR, 98 %, Adamas-beta), HfO_2 (AR, 98 %, Macklin), and hydrofluoric acid (37%, Aladdin) are commercially purchased without further refinement.

1.2 Syntheses of KBZFC and KBHFC. The polycrystalline samples of KBZFC and KBHFC were synthesized by the hydrothermal reaction. For KBZFC, a mixture of KCl (1 mmol, 74.6 mg), $BaCl_2 \cdot 2H_2O$ (1.5 mmol, 366.5 mg), and ZrF_4 (2 mmol, 344.4 mg) was added into the 20 mL Teflon-lined vessel, with 3 ml deionized water and 1 ml HF as solvent. The liner was sealed into matched stainless-steel case, placed in an oven, heated to 210 °C for 3 h, kept for 3 days, finally cooled to room temperature at the rate of 2 °C h^{-1}. The polycrystalline sample of KBHFC was obtained in similar process by changing 2 mmol ZrF_4 to 2 mmol HfO_2. Colorless block crystals of KBZFC and KBHFC were collected with the yields of 70/80 % (based on ZrF_4/HfO_2) after being filtered with suction and dried in air.

1.3 Single-Crystal Structure Determination. Clean single crystals of KBZFC and KBHFC were selected for single-crystal XRD data collection on the Bruker D8 QUEST diffractometer equipped with a CCD detector (Mo Kα radiation, λ = 0.71073 Å) at 296(2) K. Direct Method of SHELXTL program package was chosen to solve the structures,[1] and full-matrix least-squares technique was used to refine all atoms. Crystal data, cell parameters, bond valence sum (BVS) calculations for atoms,[2] and selected bond lengths for KBZFC and KBHFC are summarized in Tables S1–S3. The single-crystal structure data of KBZFC and KBHFC were also deposited with the CCDC numbers of 2283473 and 2311168.

1.4 Energy-Dispersive Spectroscopy. The existence of K, Ba, Zr/Hf, F, and Cl elements in KBZFC and KBHFC was verified by energy dispersive spectrometry (EDS) and no other elements were found.

1.5 Powder X-Ray Diffraction Analysis. The polycrystalline powder samples of KBZFC and KBHFC were ground into powder and then used for powder XRD tests with an automated Bruker D8 X-ray diffractometer at room temperature. The test range was set from 10 to 60 ° with the scan step width of 0.02 °/min. The results indicate that the experimental XRD patterns are identical with the simulated ones converted from the cif documents on Mercury program, which implies the purity of the obtained samples.

1.6 UV-vis-NIR Diffuse Reflectance and Infrared (IR) Spectroscopies. The UV-vis-NIR diffuse reflectance spectra were carried out on a Carry 5000 UV-vis-NIR spectrometer from 200 to 800 nm. Pure barium sulfate powder was used as a reference during the test. The IR spectra were collected on a Fourier transform IR spectrometer in the range of 4000–400 cm^{-1} with pure KBr powder as background.

1.7 UV-vis-NIR Transmittance Spectroscopy. UV-Vis-NIR transmittance spectra in the wavelength range of 190–800 nm were collected with high-quality single crystals on the PerkinElmer Lambda-950 UV/ vis/NIR spectrophotometer at room temperature.

1.8 Thermogravimetric Analyses. The thermogravimetric analyses (TGA) were performed from 20 to 1000 °C with the rate of 10 °C/min on the ground polycrystalline samples of KBZFC and KBHFC, with a Netzsch STA449F3 simultaneous analyzer and N_2 as protective gas.

1.9 SHG Measurements. The SHG signals for the powder samples of KBZFC and KBHFC were detected and gathered by the Q-witched Nd: YAG laser (1064 nm) based on the modified Kurtz-Perry method.[3] The polycrystalline samples were ground and sieved into six particle size ranges (25–45, 45–75, 75–110, 110–150, 150–200, and 200–250 μm) to verify the phase-matchable behaviors of KBZFC and KBHFC. The microcrystalline KDP samples in the corresponding particle size ranges were selected as benchmark and measured under the same condition.

1.10 Refractive Index Dispersion Measurements. The birefringences of KBZFC and KBHFC were obtained on a polarizing microscope (ZEISS Axio Scope. A1) under 546.1 nm light. The formula of "R = (|Ne-No|) × T = Δn × T" was used to calculate birefringence, in which R means optical path difference, Δn represents birefringence, and T refers to the thickness of the crystal.[4]

1.11 Computational Details. The energy band gaps, density of states (DOS), birefringences, and electron density difference (EDD) maps of KBZFC and KBHFC were analyzed based on density functional theory (DFT) to study the structure-property relationship detailly.[5] Using the Perdew−Burke−Ernzerhof (PBE) functional within the generalized gradient approximation (GGA), [6] the chosen orbital electrons were: K $3s^2 3p^6 4s^1$, Ba $5s^2 5p^6 6s^2$, Zr $4s^2 4p^6 4d^2 5s^2$/Hf

$5s^2 5p^6 5d^2 6s^2$, F $2s^2 2p^5$, and Cl $3s^2 3p^5$. The cutoff energy was set as 940 eV, with Monkhorst−Pack scheme set as 4 × 4 × 2 in Brillouin zone and self-consistent convergence of the total energy set as 1.0×10^{-6} eV/atom. The calculations of second-order NLO susceptibilities were based on length-gauge formalism within the independent particle approximation.[7, 8] The second-order NLO susceptibility can be expressed as

χabc L(-2ω; ω, ω) = χabc inter (-2ω; ω, ω) + χabc intra(-2ω; ω, ω) + χabc mod(-2ω; ω, ω)

where the subscript L denotes the length gauge, χabc inter, χabc intra and χabc mod give the contributions to χabc L from interband processes, intraband processes, and the modulation of interband terms by intraband terms, respectively.

Table S1. Crystal data and structure refinement parameters for KBZFC and KBHFC.

Empirical formula	**KBZFC**	**KBHFC**
Formula weight	935.01	1109.55
T/K	296(2)	296(2)
Crystal system	tetragonal	tetragonal
Space group	$P\bar{4}m2$	$P\bar{4}m2$
a/Å	5.7502(2)	5.7439(3)
c/Å	10.2521(6)	10.2541(7)
Volume/Å^3	338.98(3)	338.31(4)
Z	1	1
ρ_{calc} (g/cm^3)	4.580	5.446
μ/mm^{-1}	10.720	24.534
F(000)	410.0	474
Radiation	MoKα (λ = 0.71073)	MoKα (λ = 0.71073)
2θ range for data collection/°	3.972 to 5.93	3.972 to 54.824
Index ranges	$-7 \le h \le 5$, $-7 \le k \le 6$, $-12 \le l \le 12$	$-7 \le h \le 6$, $-7 \le k \le 5$, $-13 \le l \le 13$
Reflections collected	2424	2574
Independent reflections/Rint	427/0.0236	469/0.0385
Data/restraints/parameters	427/0/36	469/0/36
Goodness–of–fit on F^2	1.119	1.091
Final R indexes [I>=2σ (I)]	R1^a = 0.0102, wR2^b = 0.0236	R1^a = 0.0134, wR2^b = 0.0292
Final R indexes [all data]	R1^a = 0.0103, wR2^b = 0.0236	R1^a = 0.0139, wR2^b = 0.0293
Largest diff. peak/hole (e Å^{-3})	0.47/-0.32	0.95/-0.85
Flack parameter	0.29(2)	0.03(3)

^{a}R1 = $||F_o| - |F_c||/|F_o|$; ^{b}wR2 = $[w(F_o^2 - F_c^2)^2]/[w(F_o^2)^2]^{1/2}$.

Table S2. Atomic coordinates (× 10^4), equivalent isotropic displacement parameters ($U_{eq}{}^a$, $Å^2$ × 10^3), and bond valence sums for KBZFC and KBHFC.

Atom	**Wyckoff site**	***x***	***y***	***z***	$U_{eq}{}^a/Å^2$	***Bond valence sums***
			KBZFC			
Ba(1)	2*g*	10000	5000	6331.7(3)	21.47(15)	2.13
Ba(2)	1*a*	10000	10000	1000	12.81(16)	2.23
Zr(1)	2*g*	5000	10000	7554.9(5)	9.41(15)	4.00
K(1)	1*b*	5000	5000	10000	18.4(4)	0.97
Cl(1)	1*d*	10000	0	5000	23.5(5)	1.06
F(1)	2*g*	5000	10000	9632(3)	21.2(8)	0.93
F(2)	8*l*	7569(4)	7680(4)	8058.8(14)	20.2(4)	1.09
F(3)	4*k*	5000	7793(5)	6015(3)	24.9(7)	0.96
Atom	**Wyckoff site**	***x***	***y***	***z***	$U_{eq}{}^a/Å^2$	***Bond valence sums***
			KBHFC			
Ba(1)	2*g*	0	5000	3672.9(5)	19.55(18)	2.11
Ba(2)	1*a*	0	10000	10000	12.1(3)	2.25
Hf(1)	2*g*	0	5000	7559.9(3)	8.99(15)	4.12
K(1)	1*b*	5000	5000	10000	15.0(9)	0.98
Cl(1)	1*d*	0	0	5000	18.9(9)	1.08
F(1)	4*k*	-2205(8)	5000	6021(4)	22.3(11)	0.97
F(2)	8*l*	2316(5)	7564(5)	8064(2)	18.3(6)	0.82
F(3)	2*g*	0	5000	9630(4)	18.7(13)	0.95

${}^aU_{eq}$ is defined as one third of the trace of the orthogonalized U_{ij} tensor.

Table S3. Important bond lengths (Å) for KBZFC and KBHFC.

Bond	**Dist./Å**	**Bond**	**Dist./Å**
		KBZFC	
Ba(2)–F(1)	2.8997(4) × 4	Zr(1)–F(1)	2.130(3)
Ba(2)–F(2)	2.7739(17) × 8	Zr(1)–F(2)	2.056(2) × 4
Ba(1)–Cl(1)	3.18278(18) × 2	Zr(1)–F(3)	2.025(3) × 2
Ba(1)–F(2)	2.732(2) × 4	K(1)–F(1)	2.8997(4) × 4
Ba(1)–F(3)	3.3091(14) × 4	K(1)–F(2)	2.9184(17) × 8
Ba(1)–F(3)	2.721(3) × 2		
		KBHFC	
Ba(2)–F(2)	2.769(3) × 8	Hf(1)–F(3)	2.123(4)
Ba(2)–F(3)	2.8969(6) × 4	Hf(1)–F(2)	2.051(3) × 4
Ba(1)–Cl(1)	3.1743(3) × 2	Hf(1)–F(1)	2.023(4) × 2
Ba(1)–F(2)	2.740(3) × 4	K(1)–F(2)	2.913(3) × 8
Ba(1)–F(1)	3.305(2) × 4	K(1)–F(3)	2.8969(6) × 4
Ba(1)–F(1)	2.721(4) × 2		

Table S4. Summary of noncentrosymmetric halides with mixed F and Cl elements.

Compound	Space group	F/Cl	SHG intensity	UV cutoff edge
$Sb_2Cl_{6.5}F_{3.5}$[9]	*C*2	3.5:6.5	–	–
$SbCl_3F_2$[10]	*I*4	2:3	–	–
$SbF_{1.6}Cl_{3.4}$[11]	*I*4	1.6:3.4	–	–
$TaCl_4F$[12]	$I\bar{4}$	1:4	–	–
$SbCl_4F$[13]	$I\bar{4}$	1:4	–	–
$SbCl_3F_2$[14]	$I\bar{4}$	2:3	–	–
$CsSbClF_3$[15]	$I\bar{4}2m$	3:1	0.3 × KDP	405 nm
Sn_2ClF_3[16]	$P2_12_12_1$	3:1	–	–
Sn_2ClF_3[17]	$P2_13$	3:1	–	–
$Ba_{10}(MnFeF_{10.15}Cl_{0.85})_3F_{0.85}Cl_{1.15}$[18]	$P31m$	31.3:3.7	–	–
$Ba_7F_{12}Cl_2$[19]	$P\bar{6}$	12:2	–	–
$Eu_7F_{12}Cl_2$[20]	$P\bar{6}$	12:2	–	–
$Pb_7F_{12}Cl_2$[21]	$P\bar{6}$	12:2	1.6 × KDP	275 nm
$Ba_{4.669}Cl_{11.3334}F_{8.0004}$[22]	$P\bar{6}$	11.3:8	–	
$Ba_{6.89}Na_{0.16}F_{12}Cl_{0.52}Br_{1.48}$[22]	$P\bar{6}$	12:0.52	–	–
$Ba_{6.92}Na_{0.11}F_{12}Cl_{0.83}Br_{1.17}$[22]	$P\bar{6}$	12:0.83	–	–
$Ba_7F_{12}Cl_{0.98}Br_{1.02}$[22]	$P\bar{6}$	12:0.98	–	–
$Ba_7F_{12}Cl_{0.7}Br_{1.3}$[22]	$P\bar{6}$	12:0.7	–	–
$Ba_{6.963}Na_{0.068}F_{12}Cl_2$[23]	$P\bar{6}$	12:2	–	–
$Ba_{6.93}F_{12}Cl_2$[24]	$P\bar{6}$	12:2	–	–
$PbF_{1.64}C_{1.27}$[25]	$P\bar{6}$	12:2	–	–
$Ba_6EuF_{12}Cl_2$[26]	$P\bar{6}$	19:5	–	–
$Ba_{12}F_{19}Cl_5$[27]	$P\bar{6}2m$	19:5	–	–
$Ba_{12}F_{19}Cl_{4.36}Br_{0.64}$[27]	$P\bar{6}2m$	19:4.36	–	–
$Ba_{12}F_{19}Cl_{3.89}Br_{1.11}$[27]	$P\bar{6}2m$	19:3.89	–	–
$Ba_{12}F_{19}Cl_{3.01}Br_{1.99}$[27]	$P\bar{6}2m$	19:3.01	–	–
$Ba_5Cu_4F_{17}Cl$[28]	$P\bar{6}2m$	17:1	–	–

$Ba_{12}F_{19}Cl_{2.01}Br_{2.99}$[27]	$P\bar{6}2m$	19:2.01	–	–
$Ba_{12}F_{19}Cl_{2.44}Br_{2.56}$[27]	$P\bar{6}2m$	19:2.44	–	–
$K_6(BiCl_6)Cl_2(H_3F_4)$ [29]	$P6_3mc$	4:6	–	–
$ClXe(Sb_2F_{11})$[30]	$Pna2_1$	11:1	–	–
$K_2SbF_2Cl_3$[31]	$P2_12_12_1$	2:3	5.0 × KDP	309 nm
KBZFC	$P\bar{4}m2$	14:1	1.0 × KDP	194 nm
KBHFC	$P\bar{4}m2$	14:1	0.9 × KDP	192.8 nm

Table S5. Summary of noncentrosymmetric metal mixed halides.

Compound	**Space group**	**Dimension**	**IR transparent range (*μ*m)**	**UV cutoff edge (nm)**	**SHG intensity**	***Δ*n (@1064 nm)**
HgBrI[32]	$Cmc2_1$	0*D*	2.5–14	335	1.4 × KTP	–
β-HgBrCl[33]	$P2_12_12_1$	0*D*	2.5–20	366	2 × KDP	–
Hg_2Br_3I[34]	$Cmc2_1$	0*D*	2.5–14	450	0.7 × KTP	–
Hg_2BrI_3[35]	$Cmc2_1$	0*D*	2.5–14	477	1.2 × KTP	–
$Cs_2Hg_2Br_2I_4{\cdot}H_2O$[36]	*Pc*	1*D*	2.5–2.7	440	6.0 × KDP	0.08
$Cs_2HgI_2Cl_2$[37]	$P2_1$	0*D*	2.5–14	394	1.5 × KDP	0.198
$Pb_7F_{12}Cl_2$[21]	$P\bar{6}$	3*D*	2.5–20	275	1.6 × KDP	–
$Pb_7F_{12}Br_2$[38]	$P\bar{6}$	3*D*	2.5–14	287	1.5 × KDP	0.045
Rb_2CdBrI_3[39]	$Ama2$	0*D*	2.5–20	309	2.0 × KDP	0.039
$Rb_2CdBr_2I_2$[40]	$Ama2$	0*D*	2.5–14	370	4.0 × KDP	–
$K_2SbF_2Cl_3$[31]	$P2_12_12_1$	0*D*	2.5–14	309	5.0 × KDP	0.116
$CsSbF_3Cl$[15]	$I\bar{4}2m$	0*D*	–	405	0.3 × KDP	0.28
$Rb_4Sn_3Cl_2Br_8$[41]	$Cmc2_1$	1*D*	–	440	0.5 × KDP	0.23
KBZFC	$P\bar{4}m2$	0*D*	2.5–23	194	1.0 × KDP	0.12

KBHFC	$P\bar{4}m2$	0*D*	2.7–23	192.8	0.9 × KDP	0.10

Table S6. The SHG-contributed percentages of the groups/ions in KBZFC and KBHFC.

Groups/ions	SHG-contributed percentages (%)
KBZFC	
ZrF_7	60.71
Ba^{2+}	14.23
Cl^{-}	25.58
K^{+}	-0.43
KBHFC	
HfF_7	33.12
Ba^{2+}	23.33
Cl^{-}	43.81
K^{+}	-0.27

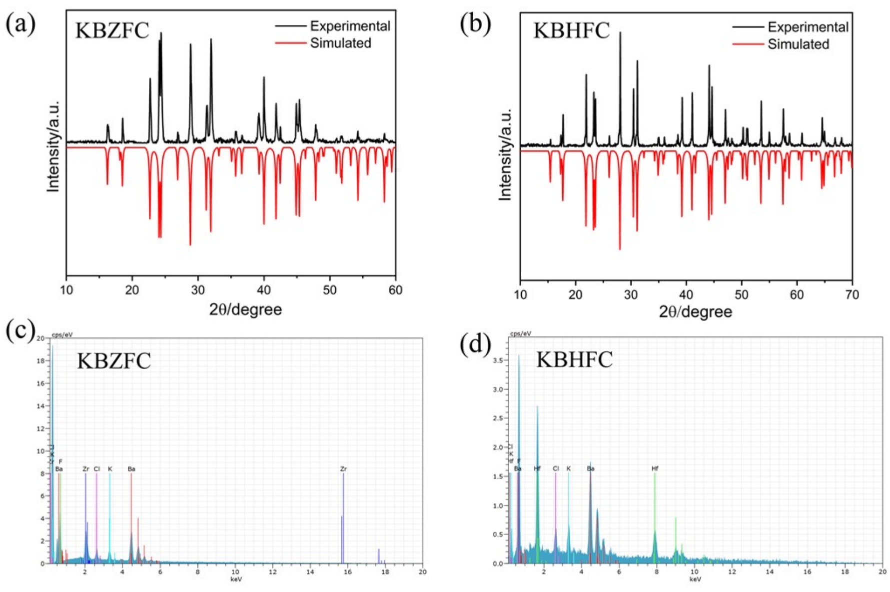

Figure S1. Powder X-ray diffraction patterns (a, b) and EDS images (c, d) for KBZFC and KBHFC.

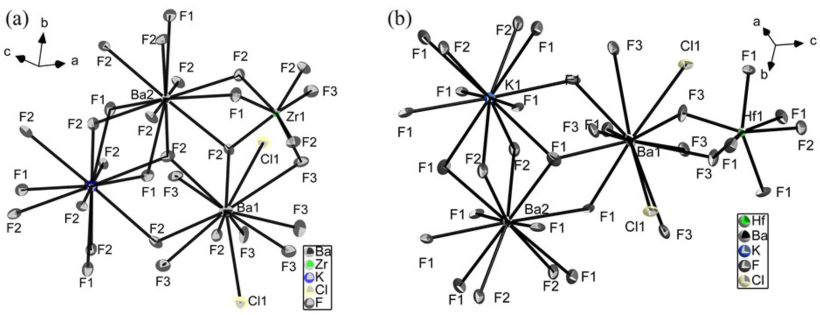

Figure S2. ORTEP-like plot of KBZFC (a) and KBHFC (b).

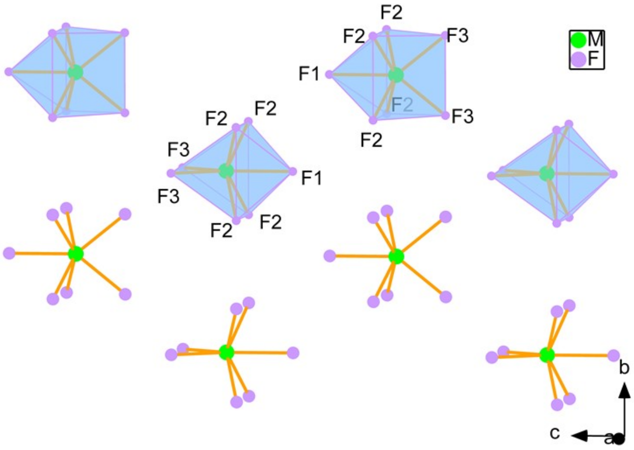

Figure S3. Arrangement of MF_7 (M = Zr, Hf) monocapped triangular prisms at *bc* plane.

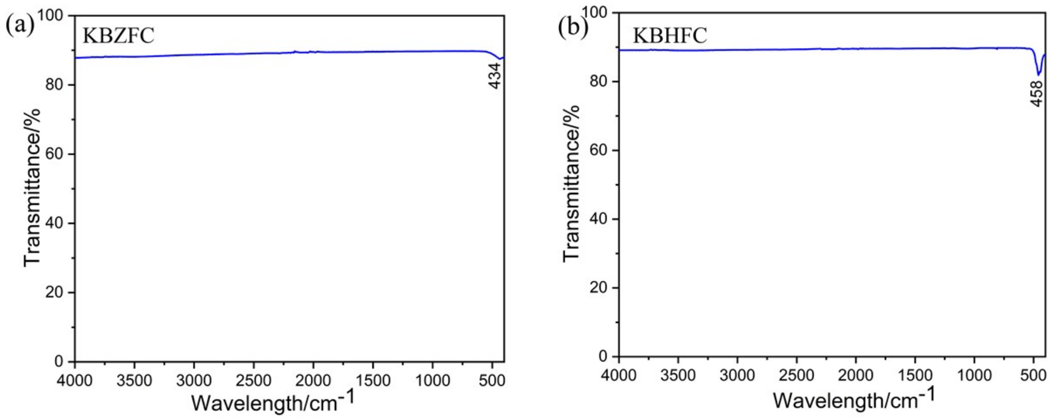

Figure S4. IR spectra of KBZFC (a) and KBHFC (b).

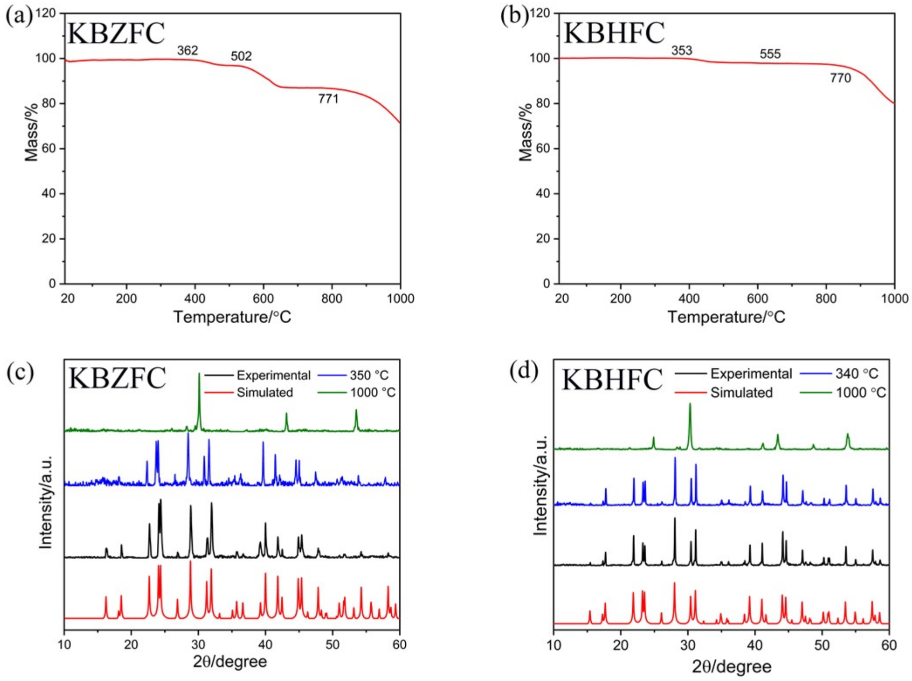

Figure S5. TG curves (a, b) and XRD analyses (c, d) of KBZFC and KBHFC.

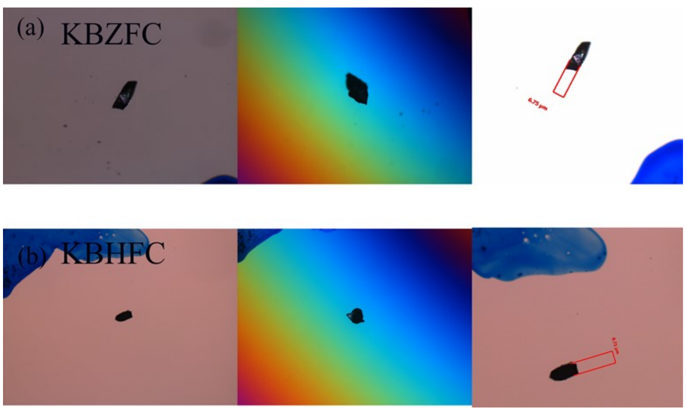

Figure S6. Photograph of crystals KBZFC (a) and KBHFC (b) for the measurement of birefringences.

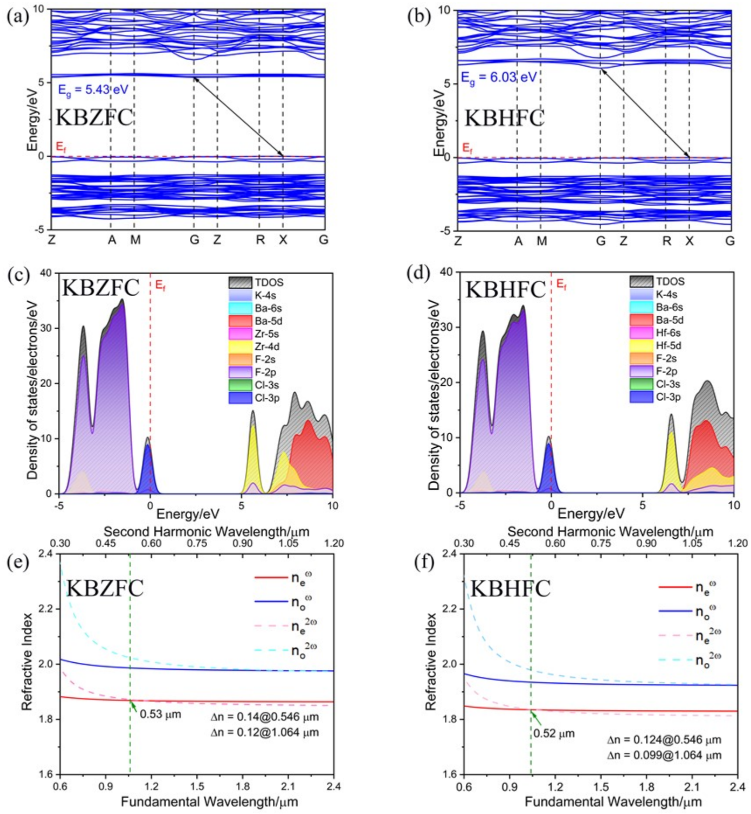

Figure S7. Calculated band structures (a, b), DOS (c, d), refractive index curves, and shortest PM wavelengths (e, f) of KBZFC and KBHFC. The Fermi level is set at 0 eV.

References

1. O. V. Dolomanov, L. J. Bourhis, R. J. Gildea, J. A. K. Howard and H. Puschmann, *J. Appl. Crystallogr.*, 2009, **42**, 339–341.
2. I. D. Brown and D. Altermatt, *Acta Crystallog. B*, 1985, **41**, 244–247.
3. S. K. Kurtz and T. T. Perry, *J. Appl. Phys.*, 1968, **39**, 3798–3813.
4. H. Y. Sha, Y. R. Shang, Z. J. Wang, R. B. Su, C. He, X. M. Yang and X. F. Long, *Small*, 2023, DOI: 10.1002/smll.202309776, e2309776.
5. M. D. Segall, P. J. D. Lindan, M. J. Probert, C. J. Pickard, P. J. Hasnip, S. J. Clark and M. C. Payne, *J. Phys-Condens. Mat.*, 2002, **14**, 2717.
6. J. C. Stewart, D. S. Matthew, J. P. Chris, J. H. Phil, I. J. P. Matt, R. Keith and C. P. Mike, *Z. Kristallogr. - Cryst. Mater.*, 2005, **220**, 567–570.
7. J. E. Sipe and E. Ghahramani, *Phys. Rev. B*, 1993, **48**, 11705–11722.
8. S. Sharma, J. K. Dewhurst and C. Ambrosch-Draxl, *Phys. Rev. B*, 2003, **67**, 165332.
9. J. G. Ballard, T. Birchall and D. R. Slim, *J. Chem. Soc., Dalton Trans.*, 1979, 62–65.
10. J. G. Ballard, T. Birchall and D. R. Slim, *J. Chem. Soc., Dalton Trans.*, 1977, 1469–1472.
11. U. Müller and Die Kristallstruktur, *Z. Anorg. Allg. Chem.*, 1979, **454**, 75–81.
12. H. Preiss, *Z. Anorg. Allg. Chem.*, 1966, **346**, 272–278.
13. M. Rolf, K. Detlef and P. Hans, *Z. Naturforsch. B*, 1994, **49**, 1–4.
14. R. Minkwitz, A. Kornath and H. Preut, *Z. Anorg. Allg. Chem.*, 1994, **620**, 638–641.
15. P. F. Gong, Y. Yang, F. G. You, X. Y. Zhang, G. M. Song, S. Z. Zhang, Q. Huang and Z. S. Lin, *Cryst. Growth Des.*, 2019, **19**, 1874–1879.
16. J. D. Donaldson, D. R. Laughlin and D. C. Puxley, *J. Chem. Soc., Dalton Trans.*, 1977, 865–868.
17. G. Bergerhoff and L. Goost, *Acta Crystallog. B*, 1974, **30**, 1362–1363.
18. J. Darriet, V. Nazabal and J. Fompeyrine, *J. Mater. Chem.*, 1996, **6**, 1781–1784.
19. H. Hagemann, V. D’Anna, M. L. Daku and F. Kubel, *Cryst. Growth Des.*, 2012, **12**, 1124–1131.
20. O. Reckeweg, F. J. DiSalvo, S. Wolf and T. Schleid, *Z. Anorg. Allg. Chem.*, 2014, **640**, 1254–1259.
21. Q. Wu, X. Liu, F. Liang, S. R. Xu, H. B. Pi, X. Han, Y. Liu, Z. S. Lin and Y. J. Li, *Dalton Trans.*, 2019, **48**, 13529–13535.

22. A. Bernsteiner and F. Kubel, *Acta Crystallogr. C*, 2006, **62**, i41–i42.
23. H. Hagemann, T. Penhouet, A. Rief and F. Kubel, *Z. Anorg. Allg. Chem.*, 2008, **634**, 1041–1044.
24. F. Kubel, H. Bill and H. Hagemann, *Z. Naturforsch. B*, 1999, **54**, 515–518.
25. S. Merlino, M. Pasero, N. Perchiazzi and A. R. Kampf, *Am. Mineral.*, 1996, **81**, 1277–1281.
26. F. Kubel, H. Bill and H. Hagemann, *Z. Anorg. Allg. Chem.*, 2000, **626**, 1721–1722.
27. F. Kubel, H. Hagemann and H. Bill, *Z. Anorg. Allg. Chem.*, 1996, **622**, 1374–1380.
28. J. Fompeyrine, V. Nazabal, J. Darriet and G. Courbion, *Eur. J. Inorg. Chem.*, 1995, **32**, 977–995.
29. A. A. Udovenko and R. L. Davidovich, *Koord. Khim.*, 1991, **17**, 1545–1546.
30. S. Seidel and K. Seppelt, *Angew. Chem. Int. Ed.*, 2001, **40**, 4225–4227.
31. Y. Huang, X. G. Meng, P. F. Gong, Z. S. Lin, X. G. Chen and J. G. Qin, *J. Mater. Chem. C*, 2015, **3**, 9588–9593.
32. Q. Wu, Y. J. Li, H. C. Chen, K. Jiang, H. L in, C. Zhong, X. G. Chen and J. G. Qom, *Inorg. Chem. Commun.*, 2013, **34**, 1–3.
33. Y. Y. Dang, X. G. Meng, K. Jiang, C. Zhong, X. G. Chen and J. G. Qin, *Dalton Trans.*, 2013, **42**, 9893–9897.
34. Y. Huang, X. G. Meng, L. Kang, Y. J. Li, C. Zhong, Z. S. Lin, X. G. Chen and J. G. Qin, *Crystengcomm*, 2013, **15**, 4196–4200.
35. Y. J. Li, M. Wang, T. X. Zhu, X. G. Meng, C. Zhong, X. G. Chen and J. G. Qin, *Dalton Trans.*, 2012, **41**, 763–766.
36. Q. Wu, Y. Huang, X. G. Meng, C. Zhong, X. G. Chen and J. G. Qin, *Dalton Trans.*, 2014, **43**, 8899–8904.
37. G. Zhang, Y. J. Li, K. Jiang, H. Y. Zeng, T. Liu, X. G. Chen, J. G. Qin, Z. S. Lin, P. Z. Fu, Y. C. Wu and C. T. Chen, *J. Am. Chem. Soc.*, 2012, **134**, 14818–14822.
38. F. Kubel and H. Völlenkle, *Solid State Sci.*, 2000, **2**, 193–196.
39. Q. Wu, X. Liu, Y. S. Du, C. L. Teng and F. Liang, *J. Mater. Chem. C*, 2020, **8**, 9005–9011.
40. Q. Wu, X. G. Meng, C. Zhong, X. G. Chen and J. G. Qin, *J. Am. Chem. Soc.*, 2014, **136**, 5683–5686.
41. P. F. Gong, S. Y. Luo, Y. Yang, F. Liang, S. Z. Zhang, S. G. Zhao, J. H. Luo and Z. S. Lin, *Cryst. Growth Des.*, 2018, **18**, 380–385.